



저작자표시-비영리-변경금지 2.0 대한민국

이용자는 아래의 조건을 따르는 경우에 한하여 자유롭게

- 이 저작물을 복제, 배포, 전송, 전시, 공연 및 방송할 수 있습니다.

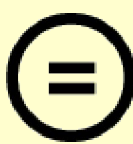
다음과 같은 조건을 따라야 합니다:



저작자표시. 귀하는 원 저작자를 표시하여야 합니다.



비영리. 귀하는 이 저작물을 영리 목적으로 이용할 수 없습니다.



변경금지. 귀하는 이 저작물을 개작, 변형 또는 가공할 수 없습니다.

- 귀하는, 이 저작물의 재이용이나 배포의 경우, 이 저작물에 적용된 이용허락조건을 명확하게 나타내어야 합니다.
- 저작권자로부터 별도의 허가를 받으면 이러한 조건들은 적용되지 않습니다.

저작권법에 따른 이용자의 권리와 책임은 위의 내용에 의하여 영향을 받지 않습니다.

이것은 [이용허락규약\(Legal Code\)](#)을 이해하기 쉽게 요약한 것입니다.

[Disclaimer](#)



**Comparative Study on Mechanical Performance of
SLA-Based Titanium Dental Implants with
Additional Surface Treatments**

Yoo, Jungmin

**Department of Industrial Dentistry
Graduate School
Yonsei University**

**Comparative Study on Mechanical Performance of
SLA-Based Titanium Dental Implants with
Additional Surface Treatments**

Advisor Kim, Jee-Hwan, D.D.S., M.S.D., Ph.D.

**A Master's Thesis Submitted
to the Department of Industrial Dentistry
and the Committee on Graduate School
of Yonsei University in Partial Fulfillment of the
Requirements for the Degree of
Master of Applied Life Science**

Yoo, Jungmin

June 2025

**Comparative Study on Mechanical Performance of
SLA-Based Titanium Dental Implants with
Additional Surface Treatments**

**This Certifies that the Master's Thesis
of Yoo, Jungmin is Approved**

Committee Chair Oh, Kyung Chul

Committee Member Kim, Jee-Hwan

Committee Member Lee, Hyeonjong

**Department of Industrial Dentistry
Graduate School
Yonsei University
June 2025**

감사의 글

2년간의 석사 과정을 마무리하며, 본 논문이 완성되기까지 저를 이끌어 주시고 격려해주신 모든 분께 이 지면을 빌려 깊은 감사의 말씀을 올립니다.

먼저, 논문의 주제 선정부터 연구의 전 과정에 이르기까지 아낌없는 지도와 따뜻한 격려로 큰 힘이 되어 주신 김지환 교수님께 진심으로 감사의 마음을 전합니다. 교수님의 세심한 조언과 변함없는 관심이 없었다면 본 논문을 완성하는 데 많은 어려움이 있었으리라 생각합니다. 아울러, 연구의 방향을 함께 고민해주시고, 날카로운 통찰과 세밀한 지도로 논문의 완성도를 높여 주신 오경철 교수님과 이현종 교수님께도 깊은 감사를 드립니다. 또한 바쁘신 일정에도 불구하고 연구의 여러 과정에서 실질적인 도움을 아끼지 않으신 김성로 선임연구원님, 한재원 주임연구원님, 최고은 선임연구원님, 노건호 선임연구원님께도 진심으로 감사의 말씀을 전합니다. 여러 연구원님의 조언과 지원이 있었기에 본 연구가 열매를 맺을 수 있었습니다.

지난 9년간 오스템임플란트 인허가실에서의 경험은 저에게 매우 소중한 배움의 시간이었습니다. 특히, 대학원 진학이라는 소중한 기회를 주시고, 늘 따뜻한 격려와 지원을 아끼지 않으신 손희권 실장님께 깊은 감사의 말씀을 드립니다. 그리고 일과 학업을 병행할 수 있도록 세심한 배려와 지원을 보내주신 배진우 팀장님께도 진심으로 감사드립니다. 더불어, 언제나 따뜻한 격려와 응원을 아끼지 않으신 직장 내 선후배와 동료분들, 석사 과정 중 여러 어려움 속에서도 든든한 조언과 지지로 큰 힘이 되어 주신 치의학산업학과의 선후배, 그리고 동기분들께도 감사의 마음을 전합니다. 여러분과 함께한 소중한 인연을 오래도록 간직하며, 앞으로 각자의 자리에서 의미 있는 성취와 기쁨이 늘 함께하시기를 진심으로 바랍니다.

마지막으로, 이 모든 과정을 끝까지 완주할 수 있도록 한결같은 사랑과 믿음으로 저를 응원해주신 부모님과 동생에게 이 자리를 빌려 진심으로 감사의 마음을 전합니다.

2025년 6월

유정민

TABLE OF CONTENTS

LIST OF FIGURES	iii
LIST OF TABLES	iv
ABSTRACT IN ENGLISH	v
1. INTRODUCTION	1
1.1. Background of the Study	1
1.1.1. Regulatory Frameworks	2
1.1.2. Surface Modifications and Mechanical Testing	3
1.2. Objective of the Study	4
2. MATERIALS AND METHODS	5
2.1. Specimen Preparation Methodology	5
2.1.1. Mechanical Test Preparation: Fixation of Specimen	11
2.2. Evaluation Standard: ISO 14801:2016	15
2.3. Testing Protocol: Static Compression Test	16
2.4. Testing Protocol: Dynamic Loading Test	17
2.5. Statistical Analysis	18
3. RESULTS	19
3.1. Static Compressive Strength from Static Compression Test	19
3.2. Fatigue Limit from Dynamic Loading Test	24
4. DISCUSSION	29
5. CONCLUSION	33
REFERENCES	34



ABSTRACT IN KOREAN	38
--------------------------	----

LIST OF FIGURES

<Fig 1> Surface morphology of each dental implant used for this study.	9
<Fig 2> Components of implant-abutment assemblies for this study.	10
<Fig 3> Feature of fixation of specimen.	11
<Fig 4> Dual column universal testing machine for static compression test.	12
<Fig 5> Linear-torsion testing machine for dynamic loading test.	12
<Fig 6> Specimen loading test configuration.	14
<Fig 7> Specimen set-up for static compression and dynamic loading test.	16
<Fig 8> Time-load diagram and specimens after static compression test with Group A (TSIII SA Implant).	21
<Fig 9> Time-load diagram and specimens after static compression test with Group B (TSIII BA Implant).	22
<Fig 10> Time-load diagram and specimens after static compression test with Group C (TSIII SOI Implant).	23
<Fig 11> S-N curve and specimens after dynamic loading test with Group A (TSIII SA Implant).	26
<Fig 12> S-N curve and specimens after dynamic loading test with Group B (TSIII BA Implant).	27
<Fig 13> S-N curve and specimens after dynamic loading test with Group C (TSIII SOI Implant).	28



LIST OF TABLES

<Table 1> Features of implant and abutment used in this study.	6
<Table 2> Values of the static compression tests.	20
<Table 3> Values of the dynamic loading tests.	25
<Table 4> Performance criteria of the static compressive strength and fatigue limit from regulatory guidance document in South Korea.	31
<Table 5> Performance criteria of the fatigue limit from regulatory guidance document in United States.	31

ABSTRACT

Comparative Study on Mechanical Performance of SLA-Based Titanium Dental Implants with Additional Surface Treatments

This study aimed to evaluate whether secondary surface treatments applied to sandblasted, large-grit, acid-etched (SLA) surfaced commercially pure titanium (CP-Ti) implants induce differences in mechanical performance.

A total of 33 implant-abutment assemblies with identical dimensions (3.75 mm diameter, 10 mm length) and internal hex connection type were divided into three groups: Group A (control; TSIII SA Implant, OSSTEM IMPLANT; SLA surface), Group B (TSIII BA Implant, OSSTEM IMPLANT; SLA surface coating with hydroxyapatite (HA), glucose and NaCl at saline concentrations), and Group C (TSIII SOI Implant, OSSTEM IMPLANT; SLA surface coating with hydroxy-ethyl piperazine ethane sulfonic acid (HEPES)). Static compression and dynamic loading tests were performed according to ISO 14801:2016 standard.

The static compressive strength was measured as 488.7 ± 17.23 N for Group A, 456.4 ± 8.82 N for Group B, and 488.8 ± 31.27 N for Group C. Statistical analysis demonstrated no significant differences ($p > 0.05$) in static compressive strength among the test groups, suggesting that additional surface treatments beyond the SLA process did not substantially enhance the static mechanical performance. Under cyclic loading simulating clinical masticatory conditions, all groups endured 5 million cycles at their respective thresholds: Group A at 210 N (43% of specified maximum load), Group B at 233 N (51%), and Group C at 210 N (43%). These results establish the fatigue limits that meet the requirements of major regulatory bodies (e.g., MFDS, FDA): 210 N for Group A and C, 233 N for Group B. From the results of dynamic loading tests, the weakest point in

all implant-assemblies was consistently located 3 mm apical to the nominal bone level, corresponding to the fixation area mimicking 3 mm of marginal bone loss.

The results indicated that various surface treatments addition to SLA titanium implants did not significantly impact the static and dynamic mechanical properties. All tested implants demonstrated performance that exceeded regulatory standards, suggesting that different surface treatments intended to enhance biological osseointegration can be applied without compromising mechanical stability.

Key words: dental implants, surface treatment, mechanical characterization, static compressive strength, fatigue limit

1. INTRODUCTION

1.1. Background of the Study

Dental implants have undergone significant advancements since their introduction by Bränemark in the 1960s. Initially, they were primarily utilized for edentulous patients to improve denture retention, stability, functional efficiency, and overall quality of life. Over time, their applications have expanded to include fully edentulous, partially edentulous, and single-tooth loss patients, becoming a cornerstone of modern prosthetic dentistry (Adell et al., 1990; Adell et al., 1981; Albrektsson, 1988; Albrektsson et al., 1987; Albrektsson et al., 1988; Albrektsson et al., 1986; Won et al., 2010).

To ensure safe and effective use in diverse clinical applications, dental implants must meet stringent regulatory requirements set by national authorities. Premarket approval processes require manufacturers to demonstrate compliance with international standards, particularly *ISO 10993 Biological evaluation of medical devices* for biological safety and *ISO 14801 Dentistry – Implants – Dynamic loading test for endosseous dental implants* for fatigue performance evaluation. These standards provide critical frameworks for evaluating the safety and mechanical reliability of dental implants.

1.1.1. Regulatory Frameworks

The ISO 10993 series outline protocols for assessing the biocompatibility of medical devices, including dental implants. It evaluates potential adverse reactions such as cytotoxicity, sensitization, irritation, and carcinogenic risks (International Organization for Standardization, 2018). Compliance with ISO 10993 ensures that implant materials do not elicit harmful responses when in contact with human tissues, facilitating safe integration into the body without causing inflammation or rejection.

ISO 14801 specifies methods for fatigue testing of endosseous dental implants under simulated "worst-case" conditions. This standard evaluates mechanical durability by subjecting implants to cyclic loading that mimics functional stresses experienced during mastication. Fatigue testing measures the implant's ability to withstand repeated forces over up to five million cycles, providing insights into its long-term structural integrity (International Organization for Standardization, 2016). With its limitation on artificial testing environment, however, ISO 14801 focuses exclusively on primary mechanical fixation, which refers to the initial stability achieved by implant placement. It does not account for secondary biological fixation, which arises from bone remodeling and osseointegration over time (Smeets et al., 2016).

1.1.2. Surface Modifications and Mechanical Testing

Surface modifications on titanium implants, such as roughened textures or bioactive coatings, are widely used to accelerate osseointegration and secondary stability (Smeets et al., 2016). These treatments improve bone apposition and promote biological integration but may introduce mechanical variables that could affect fatigue performance under ISO 14801 testing conditions. For instance, surface treatments like acid etching can create micro-pits that act as stress concentrators, potentially reducing fatigue resistance, while sandblasting may introduce compressive residual stresses that enhance mechanical durability (Ding et al., 2018; Pazos et al., 2010).

Despite these potential effects, ISO 14801 isolates primary mechanical fixation by excluding biological factors such as bone regeneration and soft tissue interactions. Consequently, implants with different surface treatments but identical geometries and prosthetic connections are hypothesized to exhibit comparable fatigue performance under ISO 14801-compliant evaluations.

This study was conducted to address this gap by investigating whether surface modifications intended for biological fixation influenced both static and dynamic mechanical properties, including fatigue outcomes under ISO 14801 testing parameters. By evaluating implants with varying surface treatments under identical quasi-static and cyclic loading conditions, this research was aimed at determining whether their static compressive strength and dynamic fatigue resistance remained equivalent despite differences in osseointegration potential.

1.2. Objective of the Study

This study was conducted to evaluate whether secondary surface treatments applied to sandblasted, large-grit, acid-etched (SLA) surfaced commercially pure titanium (CP-Ti) implants induced differences in mechanical performance. The SLA surface, which is recognized as the clinical gold standard for dental implants due to its optimal balance of osseointegration potential and surface stability, served as the baseline for comparing secondary treatments (Hao et al., 2021; Lee et al., 2021).

To achieve this objective, the static compressive strength and fatigue limit of implants with identical dimensions (diameter and length) but differing surface treatments applied to SLA-based CP-Ti materials were assessed.

The null hypothesis of this study was that there were no differences in primary mechanical performance between SLA-surfaced titanium implants and those with additional secondary surface treatments applied to the same SLA surface.



2. MATERIALS AND METHODS

2.1. Specimen Preparation Methodology

The dental implants and abutments evaluated in this study were systematically documented in Table 1, which provided key specifications including geometric parameters and surface modifications protocols, and materials details. For the dental implants, three commercially available different types of implants were used, all having identical internal hex connection type and dimensions but differing in the surface treatments applied to the SLA-based surface, in order not to differentiate the physical properties of specimens used.

Table 1. Features of implant and abutment used in this study.

Implant Diameter (Ø)	Implant Length (mm)	Connection	Group Type Classification	Material		
				Implant	Surface Treatment Basis	Abutment and Additional Abutment Screw
Group A						
3.75	10	Internal Hex Connection	(TSIII SA Implant, Test group)	CP-Ti Grade 4	Sandblasted, large-grit, acid-etched (SLA)	None Calcium phosphate (hydroxyapatite (HA)) by immersion and hydrophilic materials (glucose and NaCl with saline concentrations) coating Hydrophilic material (hydroxy-ethyl piperazine ethane sulfonic acid (HEPES)) coating
Group B						
			(TSIII BA Implant, Test group)			Ti-6Al-4V ELI
Group C						
			(TSIII SOI Implant, Test group)			

Manufacturer: OSSSTEM IMPLANT, Busan, Korea.

For dental implants, a representative TS system implant with an internal hexagonal connection was selected. Among the surface treatment options available for this given system, TSIII SA Implant, TSIII BA Implant, and TSIII SOI Implant were chosen:

TSIII SA Implant was subjected to a sandblasted, large-grit, acid-etched (SLA) surface treatment process in which alumina (Al_2O_3) powder was first used to sandblast the titanium surface, creating macro-roughness, and this was followed by acid etching with a mixed solution of hydrochloric acid (HCl) and sulfuric acid (H_2SO_4), which generated microscale crater pits. As a result, a uniformly roughened surface with an average roughness (Ra) of 1.8-3.0 μm was achieved across the implant. This implant was assigned to Group A as a control group for this study.

TSIII BA Implant was manufactured with the same SLA surface treatment as TSIII SA Implant, achieving uniform surface roughness ($\text{Ra} = 1.8\text{-}3.0 \mu\text{m}$). A thin hydroxyapatite (HA) layer was coated via calcium phosphate (Ca/P) solution immersion on to this SLA surface. This HA coating was designed to be resorbable by osteoclasts during bone remodeling, enabling bonding between newly formed lamellar bone and titanium surface. Additionally, a protective hydrophilic layer was applied using a glucose-saline solution to prevent the absorption of airborne contaminants, such as hydrocarbons particles, and maintain surface hydrophilicity. This implant was assigned to Group B as one of test groups for this study.

TSIII SOI Implant was manufactured with the same SLA surface treatment as TSIII SA Implant, resulting in a uniform surface roughness ($\text{Ra} = 1.8\text{-}3.0 \mu\text{m}$). To prevent the absorption of airborne contaminant, such as hydrocarbons particles, and to maintain surface hydrophilicity, the surface was coated with hydroxy-ethyl piperazine ethane sulfonic acid (HEPES), a type of acid-based buffer solution. This implant was assigned to Group C as another test group for this study.

For dental abutment (and abutment screw), TS Transfer Abutment, a screw- and cement-retained prosthesis was selected. This abutment was designed with a hexagonal connection that was



made to be compatible with all three implants used in this study.

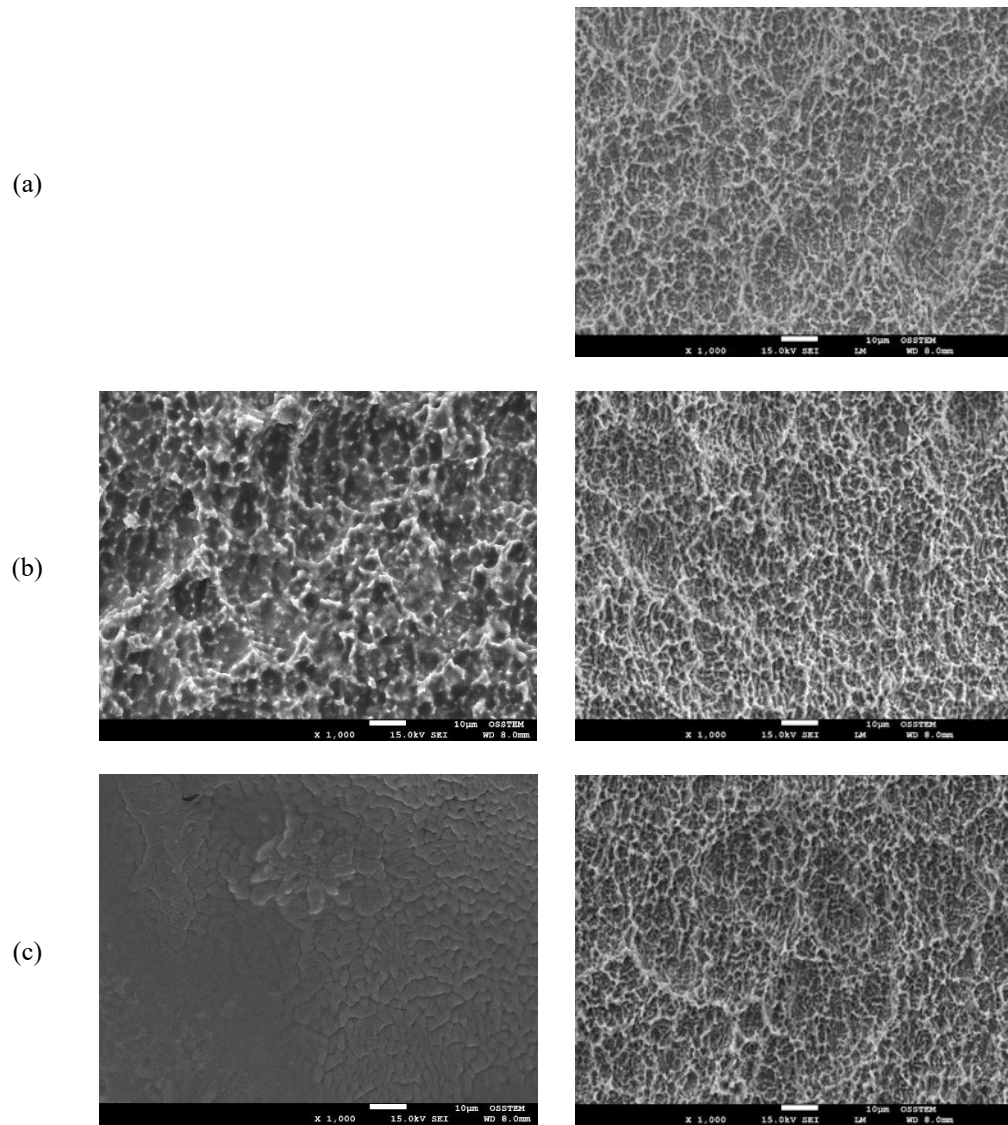


Figure 1. Surface morphology of each dental implant used for this study. (a) TSIII SA Implant with SLA surface treatment, (b) TSIII BA Implant with SLA surface treatment and additional HA and glucose-saline solution coating (left: image taken after all surface treatment, right: imaged after removal of the hydrophilic material coating), and (c) TSIII SOI Implant with SLA surface treatment and additional HEPES coating (left: image taken after all surface treatment, right: imaged after

removal of the hydrophilic material coating).

This study evaluated thirty-three implant-abutment assemblies, each comprising a titanium implant, mating abutment, and fixation screw sourced from OSSTEM IMPLANT (Busan, Korea). As illustrated in Figure 2, all tested configurations featured internal hexagonal connections between components. The implants shared identical geometric parameters: 10 mm length, 3.75 mm outer diameter, and screw threads with 0.8 mm pitch spacing.

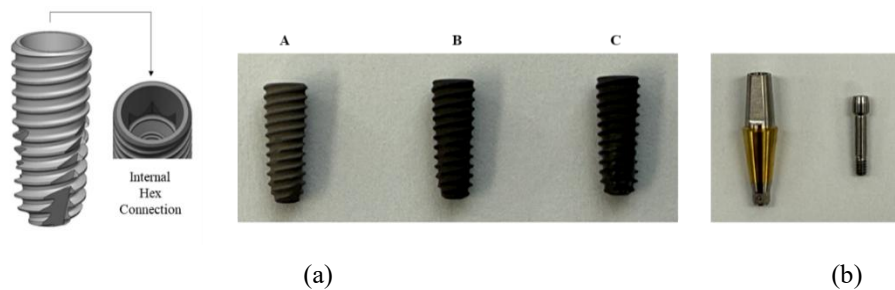


Figure 2. Components of implant-abutment assemblies for this study. (a) Implant A (TSIII SA Implant, TS3M3510S), B (TSIII BA Implant, TS3M3510B), C (TSIII SOI Implant, TS3M3510A) with 3.75 mm of diameter and 10 mm of length and (b) abutment (TS Transfer Abutment, TSTA4771TH) with 4.6 mm of diameter, 7.0 mm of abutment height and gingival height and 0° angulation; and abutment screw with 2.2 mm of diameter and 10.2 mm of length.

The experimental protocol involved thirty-three implant-abutment complexes allocated to two distinct mechanical evaluations. Fifteen specimens underwent static compression test, evenly distributed across three experimental cohorts (five per Group A, B, and C). Eighteen remaining assemblies were assigned to dynamic loading test, with six per test groups. Abutment fixation was achieved using manufacturer- recommended 20 Ncm torque, applied with a calibrated digital torque instrument (MTT03-12, MARK-10, NY, USA).

2.1.1. Mechanical Test Preparation: Fixation of Specimen

To simulate 3 mm of marginal bone resorption and to ensure consistent fixation of the implant specimen during static compression test and dynamic loading tests under 30° inclined loading, the implant was embedded in a material with an elastic modulus exceeding 3 GPa, as illustrated in Figure 3. This embedding process prepared the implant for use in all subsequent tests. The embedding material consisted of polyester resin (LS-245, Aekyung Chemical Co., Ltd., Cheongyang-gun, Korea). After embedding, the resin was left to cure completely at ambient temperature for at least 24 hours.

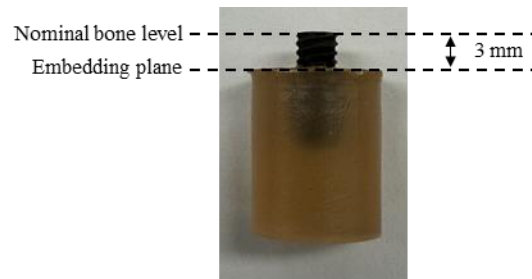


Figure 3. Feature of fixation of specimen.

For the static compression test via monotonic loading (see Figure 4), a dual column universal testing device (INSTRON 3365, Instron Corporation, MA, USA) was employed. Conversely, dynamic loading test (see Figure 5) was conducted using a linear-torsion testing apparatus INSTRON E3000, Instron Corporation, MA, USA).



Figure 4. Dual column universal testing machine for static compression test (INSTRON 3365, Instron Corporation, MA, USA).



Figure 5. Linear-torsion testing machine for dynamic loading test (INSTRON E3000, MA, USA).

All mechanical testing procedures for the dental implant system were carried out in accordance with ISO 14801:2016 standard. A loading apparatus with a hemispherical contact point, designed to resist deformation, was positioned at the exposed end of the implant-abutment assembly to facilitate force application. The force applied to this hemispherical surface was not restricted in the transverse plane, allowing lateral movement in line with the abutment's deflection under load.

For both static and dynamic testing, the main axis of the implant-abutment (Line D-E) was oriented at an angle of $30^\circ \pm 2^\circ$ relative to the loading direction of the test equipment (Line A-B), as illustrated in Figure 6. The intersection point of lines D-E and A-B was maintained at an 11 mm distance from the fixation area of the implant.

The distal section of the implant was stabilized using a holder, positioned 3 mm below the platform to simulate a clinical scenario where the marginal bone level is reduced apically after initial bone remodeling, as outlined in the ISO standard (International Organization for Standardization, 2016).

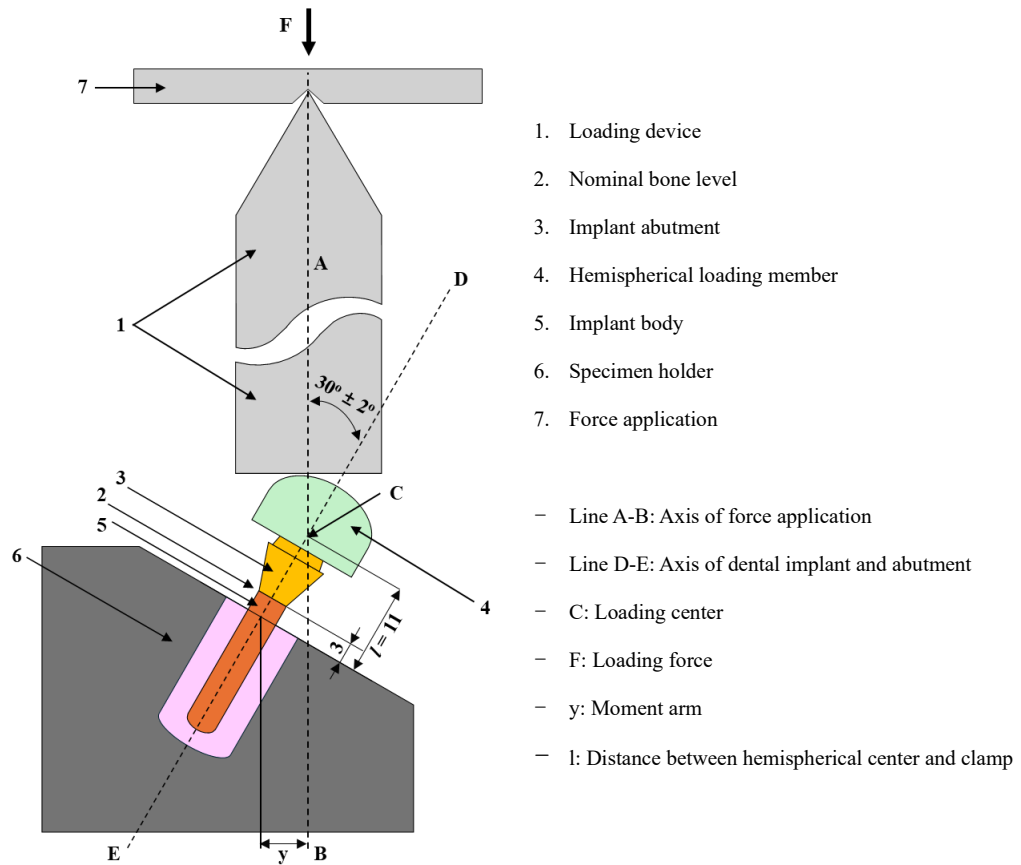


Figure 6. Specimen loading test configuration.

2.2. Evaluation Standard: ISO 14801:2016

In this study, the mechanical stability of single-tooth implant was evaluated under conditions where implant diameter, abutment angle, connection type, primary raw material, and base surface treatment were identical, but additional surface treatments differed. The assessment followed the procedures outlined in ISO 14801:2016.

The application of ISO 14801:2016 was primarily chosen as it provides a standardized evaluation framework and reflects worst-case clinical conditions. Specifically, the standard simulates lateral loading that may occur intraorally by tilting the implant at a 30° angle and mimics 3 mm of marginal bone loss during fixation. This methodology ensured consistency in testing while replicating challenging mechanical conditions encountered in clinical use (International Organization for Standardization, 2016).

Furthermore, ISO 14801:2016 is widely recognized as a regulatory standard for verifying the mechanical safety of dental implants in countries such as South Korea (MFDS) and the United States (FDA). Its adoption in this study ensured compliance with internationally accepted guidelines and facilitated the generation of reliable data for regulatory submissions.

2.3. Testing Protocol: Static Compression Test

A monotonic static compression test was initially carried on each group of specimens to determine the static compressive strength of their implant-abutment assemblies. Each of the static compression test specimens were fixed in accordance with the testing set up shown in Figure 7.

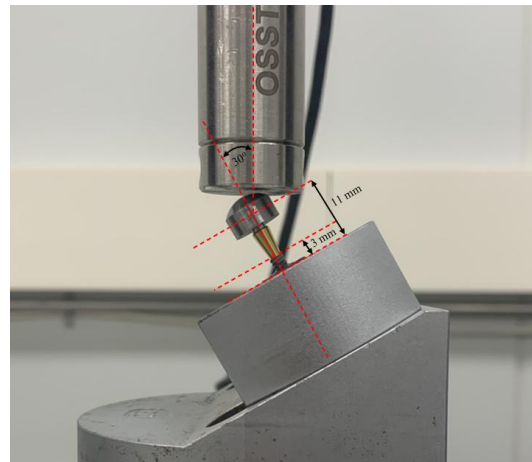


Figure 7. Specimen set-up for static compression and dynamic loading test.

The tests were performed at $20\text{ C}^{\circ} \pm 10\text{ C}^{\circ}$ in an atmospheric environment, using displacement control at a speed of 0.1 mm per minute. Each group included five assembled specimens. Failure in the static compression test was characterized as yielding, permanent deformation, loosening of the implant-abutment assembly, fracture of any part (implant, abutment, or abutment screw), or a clear drop in load resistance on the time-load curve. The highest load on the time-load curve was taken as the static compressive strength. For each group, the mean and standard deviation from five

specimens were calculated, and static compressive strengths were compared. The static compressive strength found was served as a reference for ensuing dynamic loading tests.

2.4. Testing Protocol: Dynamic Loading Test

Following the static compressive strength tests, dynamic loading tests were conducted to determine the fatigue limits of each test group. Dynamic loading test specimens were fixed using the set up shown in Figure 7, which was identical to that used in the static compression test.

For dynamic loading test under cyclic loading was performed using a sinusoidal waveform at 14 Hz frequency, oscillating between a peak load (maximum) and 10% of that peak load (minimum), following ISO 14801:2016 for air-dry condition at $20\text{ C}^\circ \pm 10\text{ C}^\circ$. Cyclic loading was applied to each implant-abutment assembly until fracture occurred or until 5×10^6 cycles were reached, (International Organization for Standardization, 2016), representing five years of clinical function (Bruno et al., 2023; Shin et al., 2009). The nominal peak load was set at 80-85% of the static compressive strength measured from earlier assessments. For each specimen, the number of cycles completed before failure was documented.

Failure criteria included structural compromised (implant, abutment, or abutment screw), irreversible shape change, disengagement of assembly, or deformation onset. The maximum endured load without failure for 5×10^6 cycles was recorded for three specimens in each test group and was referred to as the fatigue limit. The experimental data were graphically represented using stress-number of cycles to failure (S-N) curve, where applied stress levels were displayed on a linear axis and fatigue life cycles were plotted against a logarithmic scale.

2.5. Statistical Analysis

For each implant group categorized by surface treatment, static compressive strength (mean \pm standard deviation) computed from static compression tests. Intergroup comparisons required initial verification of dataset normality through the Shapiro-Wilk test, followed by variance consistency checks via Levene test. The limited dataset prompted use of a non-parametric method, Kruskal-Wallis analysis at 5% significance level ($p < 0.05$), irrespective of preliminary test outcomes. Post-hoc analysis using Mann-Whitney U test was followed as well. Statistical analyses were executed using SPSS version 27.0 software (SPSS Inc., IL, USA). Additionally, the number of cycles to fatigue fracture and the maximum endured load – referred to as the fatigue limit – acquired from the dynamic loading test were compared across groups.

3. RESULTS

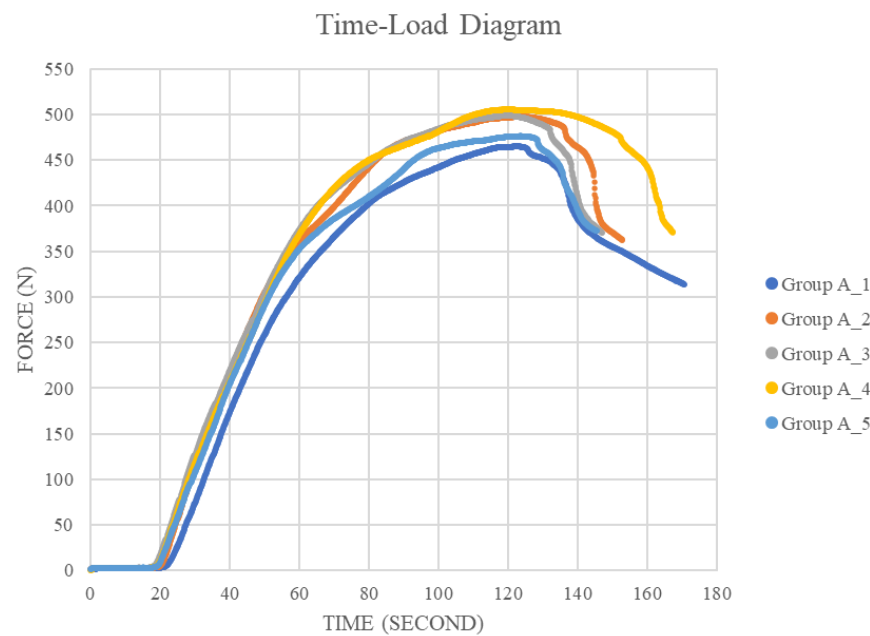
3.1. Static Compressive Strength from Static Compression Test

Static compression test outcomes for all specimens were systematically presented in Table 2. Load progression patterns across specimens were visualized through time-load diagram. The maximum peak, which corresponds to the static compressive strength, indicated the point when deformation and/or failure occurred in the implant-abutment assemblies (Figure 8-10).

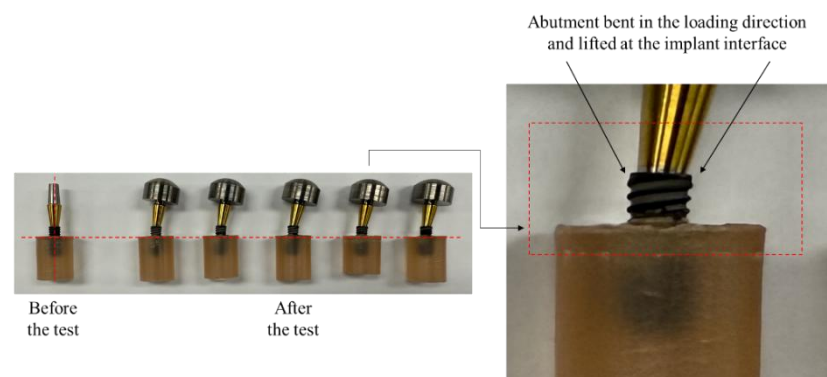
The static compressive strength for Group A (TSIII SA Implant) were 488.7 ± 17.23 N, for Group B (TSIII BA Implant) were 456.4 ± 8.82 N, and for Group C (TSIII SOI Implant) were 488.8 ± 31.27 N. The Shapiro-Wilk test confirmed that the data for each group were normally distributed (Group A: $p = 0.370$; Group B: $p = 0.061$; Group C: $p = 0.671$; all p -values > 0.05), and the Levene test confirmed the homogeneity of variances (Levene statistic with the Brown-Forsythe modification = 1.469, $p = 0.269$). Despite these findings, a non-parametric method, the Kruskal-Wallis test was performed due to the small sample size. The Kruskal-Wallis analysis revealed no statistically significant differences in median static compressive strength across groups ($H(2) = 5.420$, $p = 0.067 > 0.05$). Post-hoc pairwise comparisons using the Mann-Whitney test with Bonferroni correction (adjusted $\alpha = 0.016$) showed no significant differences between any group pairs (Group A and Group B: $p = 0.016$; Group A and Group C: $p = 0.754$; Group B and Group C: $p = 0.117$). These results indicated no statistically significant differences in static compressive strength among implants with different surface treatments under the test condition.

Table 2. Values of the static compression tests.

Specimens	Static Compressive Strength (N)		
	Group A	Group B	Group C
	(TSIII SA Implant)	(TSIII BA Implant)	(TSIII SOI Implant)
1	465.0	471.3	488.8
2	497.5	451.6	483.5
3	498.9	451.7	509.0
4	505.8	457.5	522.3
5	476.4	450.0	440.3
Mean	488.7	456.4	488.8
Standard Deviation	17.23	8.82	31.27

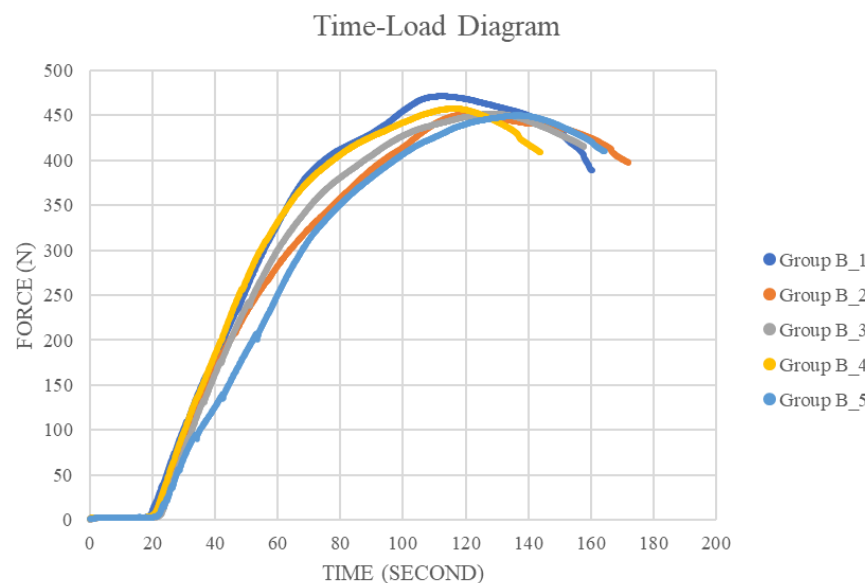


(a)

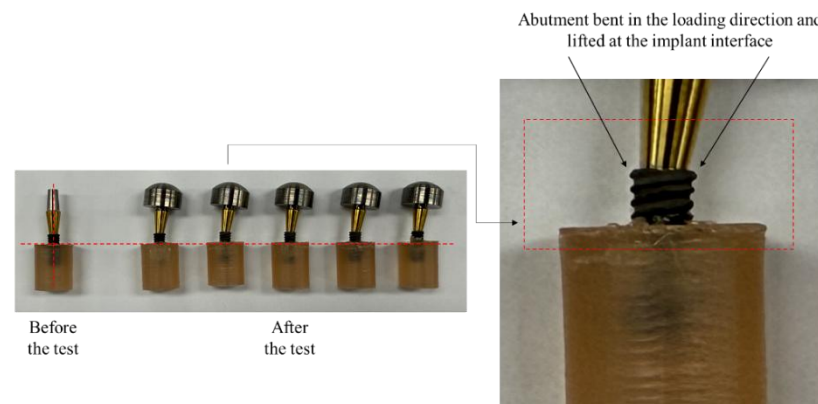


(b)

Figure 8. (a) Time-load diagram from static compression test with Group A (TSIII SA Implant) and (b) Specimens after the test.



(a)



(b)

Figure 9. (a) Time-load diagram from static compression test with Group B (TSIII BA Implant) and (b) Specimens after the test.

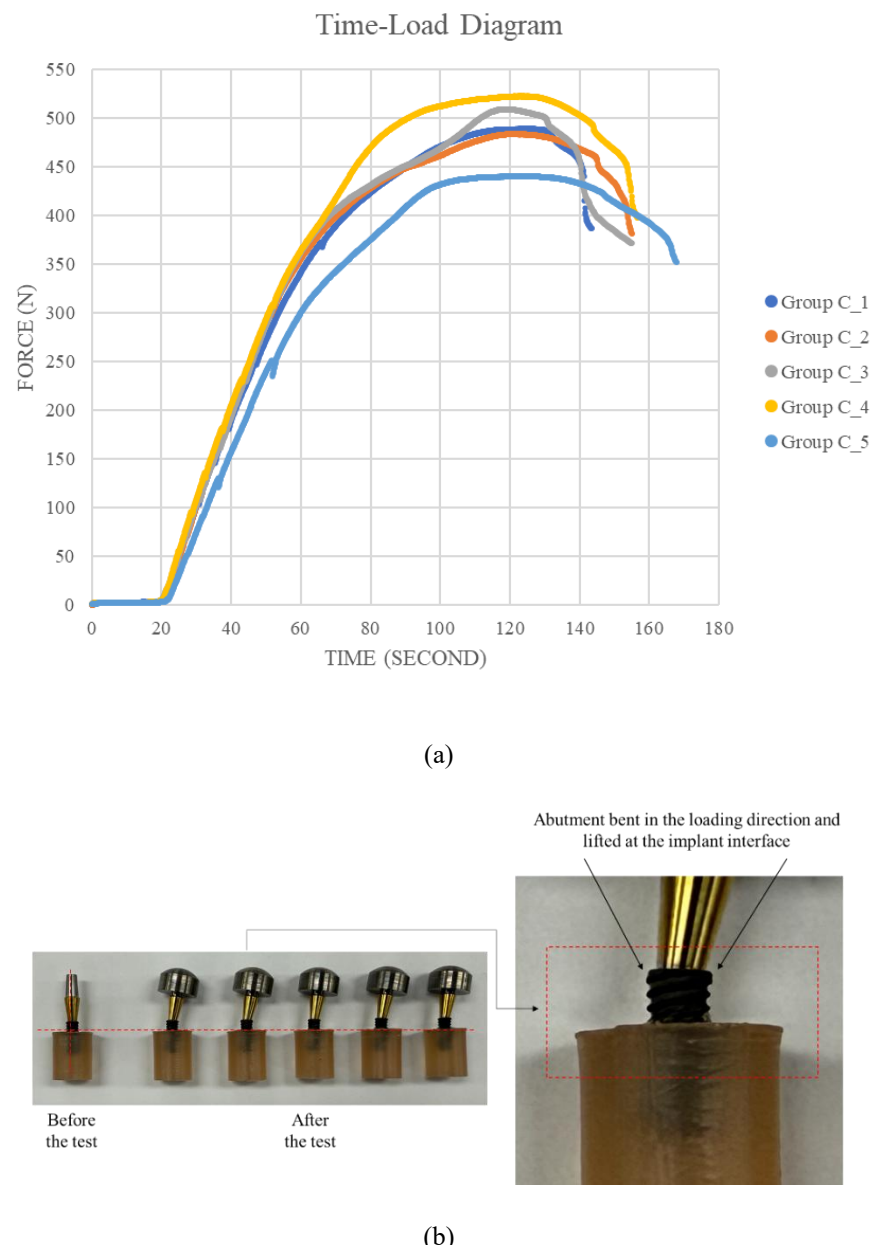


Figure 10. (a) Time-load diagram from static compression test with Group C (TSIII SOI Implant) and (b) Specimens after the test.

3.2. Fatigue Limit from Dynamic Loading Test

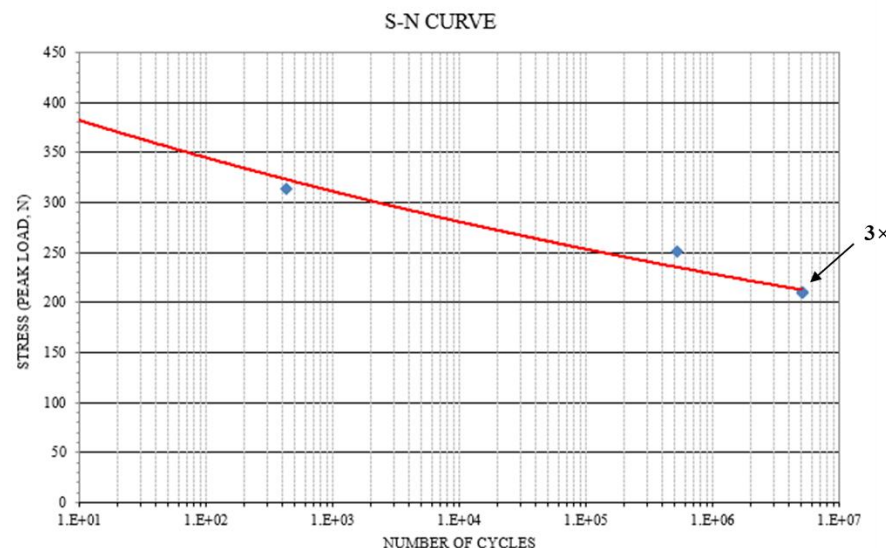
The dynamic loading test was performed starting with 80% of the mean values of static compressive strength of each test group.

Fatigue performance data were compiled in Table 3 and visualized in Figures 11-13 through stress-number of cycles to failure (S-N) curve, where the x-axis represented the logarithm of the number of cycles to failure and the y-axis showed the nominal peak load. The failure sites, as shown in the figure, were identified as transversal fracture in the threaded area along the implant body at the embedding area 3 mm below the marginal bone levels (Chrcanovic et al., 2018).

All three specimens of Group A (TSIII SA Implant) of 43% nominal peak load of 210 N withstand 5×10^6 cycles, all three specimens of Group B (TSIII BA Implant) of 51% nominal peak load of 233 N withstand 5×10^6 cycles, and all three specimens of Group C (TSIII SOI Implant) of 43% nominal peak load of 210 N withstand 5×10^6 cycles. Thus, the fatigue limit of Group A was determined to 210 N, Group B was determined to 233 N, and Group C was determined to 210 N.

Table 3. Values of the fatigue tests.

Trials	Group A	
	(TSIII SA Implant)	Total Cycle Counts
1	39.1-391.0	8
2	31.3-312.8	418
3	25.0-250.2	503,429
4	21.0-210.0	5,000,000, 5,000,000, 5,000,000
Trials	Group B	
	(TSIII BA Implant)	Total Cycle Counts
1	36.5-365.1	368
2	29.2-292.1	45,673
3	23.3-233.7	5,000,000, 5,000,000, 5,000,000
Trials	Group C	
	(TSIII SOI Implant)	Total Cycle Counts
1	39.1-391.0	16
2	31.3-312.8	597
3	25.0-250.2	374,983
4	21.0-210.0	5,000,000, 5,000,000, 5,000,000

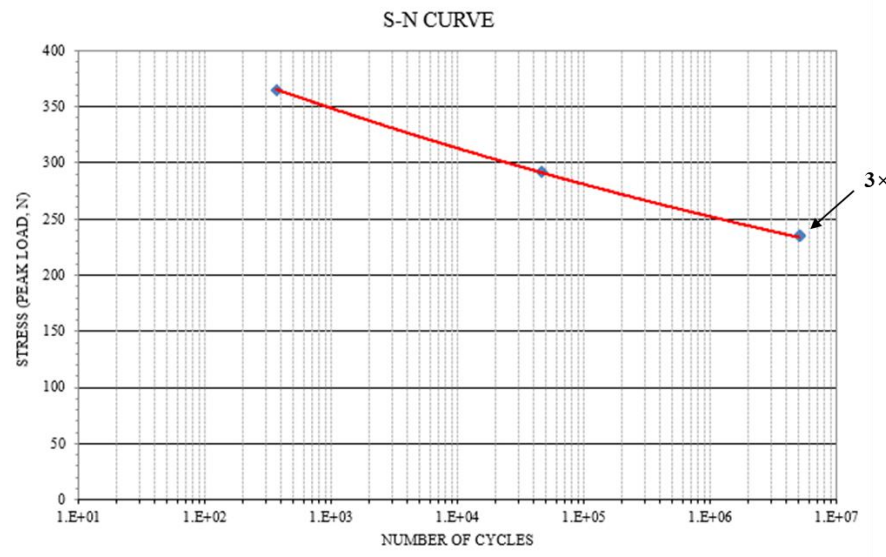


(a)

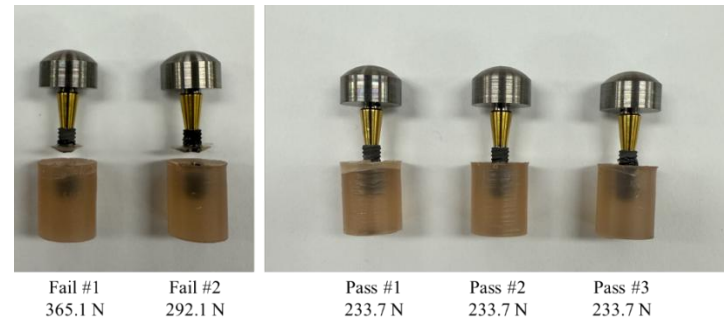


(b)

Figure 11. (a) Plotted S-N curve from dynamic loading test results for Group A (TSIII SA Implant), the loading level represented the highest peak sinusoidal load with annotated markers highlighting three specimens achieving the 5×10^6 cycles runout threshold without failure; and (b) Specimens failed and those surviving 5×10^6 cycles.



(a)



(b)

Figure 12. (a) Plotted S-N curve from dynamic loading test results for Group B (TSIII BA Implant), the loading level represented the highest peak sinusoidal load with annotated markers highlighting three specimens achieving the 5×10^6 cycles runout threshold without failure; and (b) Specimens failed and those surviving 5×10^6 cycles.

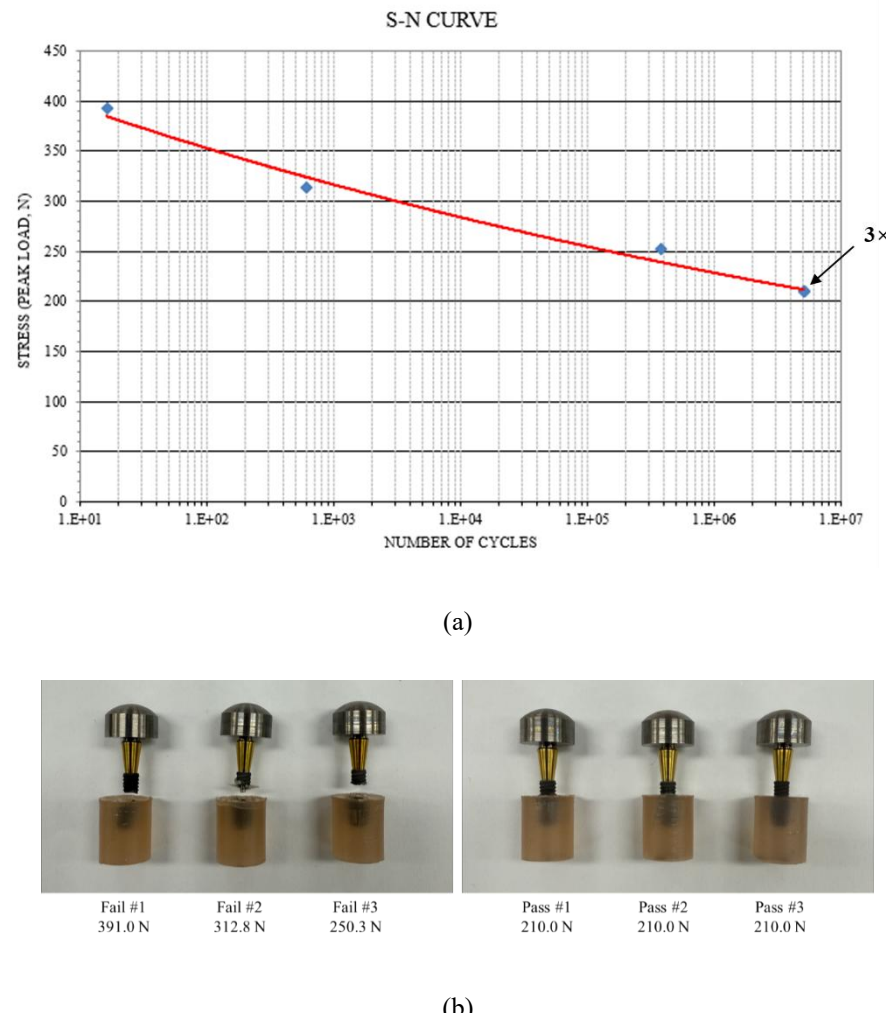


Figure 13. (a) Plotted S-N curve from dynamic loading test results for Group C (TSIII SOI Implant), the loading level represented the highest peak sinusoidal load with annotated markers highlighting three specimens achieving the 5×10^6 cycles runout threshold without failure; and (b) Specimens failed and those surviving 5×10^6 cycles.

4. DISCUSSION

The mechanical properties of dental implants are critical determinants of their clinical success and longevity (Goiato et al., 2014; Ma et al., 2022). This study evaluated the mechanical stability of single-tooth implants with identical design parameters but different surface treatments, following ISO 14801:2016 protocols.

The mechanical performance of the materials can be experimentally evaluated using static compression tests to determine static compressive strength and dynamic loading tests to identify fatigue limits. Static compressive strength refers to the fracture resistance or bearing capacity under a single application of force before failure occurs, while fatigue limit reflects its mechanical durability enduring without failure over millions of loading cycles (Sun et al., 2021). These metrics provide a comprehensive assessment of a material's resistance to both acute and repetitive mechanical stresses.

The static compressive strength was measured as 488.7 ± 17.23 N for Group A (TSIII SA Implant), 456.4 ± 8.82 N for Group B (TSIII BA Implant), and 488.8 ± 31.27 N for Group C (TSIII SOI Implant). Statistical analysis demonstrated no significant differences ($p > 0.05$) in static compressive strength among the test groups, suggesting that additional surface treatments beyond the sandblasted, large-grit, acid-etched (SLA) process did not substantially enhance static mechanical performance. Under cyclic loading simulating clinical masticatory conditions, Group A and C survived 5×10^6 cycles at 210 N, while Group B survived the same number of cycles at 233 N, thereby establishing the respective fatigue limits for each group.

The test results revealed that Group B (TSIII BA Implant), which received an additional hydroxyapatite (HA) coating combined with hydrophilic materials (glucose and NaCl with saline

concentrations) applied over the standard SLA surface treatment, exhibited slightly lower static compressive strength compared to that of the Group A (TSIII SA Implant with SLA surface treatment only) and Group C (TSIII SOI Implant with SLA surface treatment coated with hydrophilic HEPES solution). However, Group B demonstrated a marginally higher fatigue limit in dynamic loading tests.

Hydroxyapatite (HA) coatings are inherently brittle and prone to microcrack formation during static loading. These micro-defects act as stress concentrators, initiating fractures under high single-cycle loads (Family et al., 2012; Oskouei et al., 2016). Nonetheless, HA coatings create a compressive residual stress layer at the surface, which slows crack initiation and propagation under cyclic loading (Ding et al., 2018; Mukherjee et al., 2000). The HA-titanium interface absorbs energy during cyclic loading, reducing stress accumulation at critical points (Dommeti et al., 2023; Oskouei et al., 2016). Thus, it can be interpreted that HA coatings in Group B introduce micro-defects that reduce static compressive strength but enhances fatigue resistance through crack-shielding mechanisms. This trade-off aligns with studies showing HA's dual role as brittleness under static compressive single-load versus durability under dynamic cyclic load (Dommeti et al., 2023; Oskouei et al., 2016). For clinical applications, Group B's fatigue performance may suggest suitability for regions with repetitive masticatory forces, such as molar regions.

All static and fatigue values exceeded the minimum performance criteria established by regulatory authorities in South Korea (Ministry of Food and Drug Safety, 2020) and the United States (Food and Drug Administration, 2024) for endosseous dental implants (Table 4-5), indicating that all tested implant groups would be suitable for clinical applications.

Table 4. Performance criteria of the static compressive strength and fatigue limit from regulatory guidance document in South Korea (Ministry of Food and Drug Safety, 2020).

Indication	Static Compressive Strength (N)	Fatigue Limit (N)
Central/Lateral Incisor	163	110
Canine/Premolar/Molar	305	210

Table 5. Performance criteria of the fatigue limit from regulatory guidance document in United States (Food and Drug Administration, 2024).

Major Thread Diameter (mm)	Fatigue Limit (N)
3.0, 3.1, 3.2, 3.3	150
3.4, 3.5	170
3.6	180
> 3.6	200

This study adhered to the ISO 14801:2016 standard, which mandates testing under worst-case conditions. By evaluating the smallest diameter implants within the same intended use group, the results can represent the performance of the entire product line, as specified in Clause 4.3 and Annex B of the standard (International Organization for Standardization, 2016). This approach ensured that the findings have broad applicability across the range of implant dimensions available within the same system.

Despite the encouraging results, several constraints inherent to this study should be recognized. The sample size was limited to five specimens for static compression test and three specimens for dynamic loading test per test group. While this met the minimum requirement specified in ISO 14801:2016 and the results clearly exceeded regulatory requirements, a larger sample size would provide greater statistical power and potentially reveal more subtle differences between groups.

(Choi et al., 2019; Papaspyridakos et al., 2012). A further limitation stems from the fact that laboratory protocols, such as cycle counts, applied force, and loading orientation, did not fully capture the multifaceted physiological conditions in the oral environment (Choi et al., 2019). The tests were conducted on single-post endosseous dental implants, representing a worst-case scenario where masticatory loads are not distributed to adjacent teeth or implants. This approach, while methodologically sound for regulatory purposes, may not fully represent various clinical scenarios including partial or full denture applications or patients with parafunctional behaviors.

To mitigate these shortcomings, subsequent investigations are encouraged to utilize expanded sample groups, extended cycling loading programs that more closely mimic long-term clinical use, and consideration of various clinical environments and prosthetic designs. Additionally, correlating laboratory test results with long-term clinical outcomes would provide valuable insights into the predictive validity of these mechanical tests. Such comprehensive evaluation would further enhance our understanding of how different surface treatments affect the extended-duration structural integrity of dental implants in real-world clinical applications, particularly under challenging conditions such as in patients with bruxism or in posterior regions with high masticatory forces.

5. CONCLUSION

This study evaluated the mechanical performance of single-tooth implants with identical design parameters but different surface treatments additionally applied to sandblasted, large-grit, acid-etched (SLA) base surface, following ISO 14801:2016 protocols. Within the limitation of this present study, the principal findings are outlined below:

1. Static Compression Test:

Statistical analysis demonstrated no significant differences ($p > 0.05$) in static compressive strength among the test groups, suggesting that additional surface treatments beyond the SLA process did not substantially enhance the static mechanical performance.

2. Dynamic Loading Test:

Under cyclic loading simulating clinical masticatory conditions, the results establish the fatigue limits that meet the requirements of major regulatory bodies (e.g., MFDS, FDA).

3. Failure Analysis:

From the results of dynamic loading tests, the weakest point in all implant-abutment assemblies was consistently located 3 mm apical to the nominal bone level, corresponding to the fixation area mimicking 3 mm of marginal bone loss.

REFERENCES

Adell, R., Eriksson, B., Lekholm, U., Bränemark, P. I., & Jemt, T. (1990). Long-term follow-up study of osseointegrated implants in the treatment of totally edentulous jaws. *Int J Oral Maxillofac Implants*, 5(4), 347-359.

Adell, R., Lekholm, U., Rockler, B., & Bränemark, P. I. (1981). A 15-year study of osseointegrated implants in the treatment of the edentulous jaw. *International Journal of Oral Surgery*, 10(6), 387-416.

Albrektsson, T. (1988). A multicenter report on osseointegrated oral implants. *J Prosthet Dent*, 60(1), 75-84.

Albrektsson, T., Blomberg, S., Bränemark, A., & Carlsson, G. E. (1987). Edentulousness--an oral handicap. Patient reactions to treatment with jawbone-anchored prostheses. *J Oral Rehabil*, 14(6), 503-511.

Albrektsson, T., Dahl, E., Enbom, L., Engevall, S., Engquist, B., Eriksson, A. R., Feldmann, G., Freiberg, N., Glantz, P. O., Kjellman, O., & et al. (1988). Osseointegrated oral implants. A Swedish multicenter study of 8139 consecutively inserted Nobelpharma implants. *J Periodontol*, 59(5), 287-296.

Albrektsson, T., Zarb, G., Worthington, P., & Eriksson, A. (1986). The long-term efficacy of currently used dental implants: a review and proposed criteria of success. *Int J Oral Maxillofac Implants*, 1(1), 11-25.

Bruno, L., Canullo, L., Mayer, Y., Schoenbaum, T., Giuzio, F., & Maletta, C. (2023). Static and Fatigue Mechanical Performance of Abutments Materials for Dental Restorations. *Materials (Basel)*, 16(10), Article 3713.

Choi, N.-H., Yoon, H.-I., Kim, T.-H., & Park, E.-J. (2019). Improvement in Fatigue Behavior of Dental Implant Fixtures by Changing Internal Connection Design: An In Vitro Pilot

Study. *Materials*, 12(19), Article 3264.

Chrcanovic, B. R., Kisch, J., Albrektsson, T., & Wennerberg, A. (2018). Factors influencing the fracture of dental implants. *Clinical implant dentistry and related research*, 20(1), 58-67.

Ding, Q., Zhang, L., Bao, R., Zheng, G., Sun, Y., & Xie, Q. (2018). Effects of different surface treatments on the cyclic fatigue strength of one-piece CAD/CAM zirconia implants. *Journal of the Mechanical Behavior of Biomedical Materials*, 84, 249-257.

Dommeti, V. K., Pramanik, S., & Roy, S. (2023). Design of customized coated dental implants using finite element analysis. *Dental and Medical Problems*, 60(3), 385-392.

Family, R., Solati-Hashjin, M., Namjoy Nik, S., & Nemati, A. (2012). Surface modification for titanium implants by hydroxyapatite nanocomposite. *Caspian J Intern Med*, 3(3), 460-465.

Food and Drug Administration. (2024). Endosseous Dental Implants and Endosseous Dental Implant Abutments – Performance Criteria for Safety and Performance Based Pathway.

Goiato, M. C., dos Santos, D. M., Santiago, J. F., Jr., Moreno, A., & Pellizzer, E. P. (2014). Longevity of dental implants in type IV bone: a systematic review. *Int J Oral Maxillofac Surg*, 43(9), 1108-1116.

Hao, C. P., Cao, N. J., Zhu, Y. H., & Wang, W. (2021). The osseointegration and stability of dental implants with different surface treatments in animal models: a network meta-analysis. *Sci Rep*, 11(1), Article 13849.

International Organization for Standardization. (2016). *ISO 14801: Dentistry — Implants — Dynamic loading test for endosseous dental implants*. In. Geneva, Switzerland: International Organization for Standardization.

International Organization for Standardization. (2018). *ISO 10993-1: Biological evaluation of medical devices – Part 1: Evaluation and testing within a risk management process*. In. Geneva, Switzerland: International Organization for Standardization.

Lee, J., Lee, J.-B., Yun, J., Rhyu, I.-C., Lee, Y.-M., Lee, S.-M., Lee, M.-K., Kim, B., Kim, P., &

Koo, K.-T. (2021). The impact of surface treatment in 3-dimensional printed implants for early osseointegration: a comparison study of three different surfaces. *Scientific Reports*, 11(1), Article 10453.

Ma, M., Li, X., Zou, L., He, J., & Zhao, B. (2022). Mechanical properties and marginal fit of prefabricated versus customized dental implant abutments: A comparative study. *Clin Implant Dent Relat Res*, 24(5), 720-729.

Ministry of Food and Drug Safety. (2020). Guideline for Fatigue Test Criteria of Dental Implants.

Mukherjee, D. P., Dorairaj, N. R., Mills, D. K., Graham, D., & Krauser, J. T. (2000). Fatigue properties of hydroxyapatite-coated dental implants after exposure to a periodontal pathogen. *J Biomed Mater Res*, 53(5), 467-474.

Oskouei, R. H., Fallahnezhad, K., & Kuppusami, S. (2016). An Investigation on the Wear Resistance and Fatigue Behaviour of Ti-6Al-4V Notched Members Coated with Hydroxyapatite Coatings. *Materials (Basel)*, 9(2), Article 111.

Papaspyridakos, P., Chen, C. J., Singh, M., Weber, H. P., & Gallucci, G. O. (2012). Success criteria in implant dentistry: a systematic review. *J Dent Res*, 91(3), 242-248.

Pazos, L., Corengia, P., & Svoboda, H. (2010). Effect of surface treatments on the fatigue life of titanium for biomedical applications. *Journal of the Mechanical Behavior of Biomedical Materials*, 3(6), 416-424.

Shin, S. A., Kim, C. S., Cho, W., Jeong, C. M., Jeon, Y. C., & Yoon, J. H. (2009). Mechanical strength of Zirconia Abutment in Implant Restoration [Mechanical strength of Zirconia Abutment in Implant Restoration]. *Journal of Dental Rehabilitation and Applied Science*, 25(4), 349-360.

Smeets, R., Stadlinger, B., Schwarz, F., Beck-Broichsitter, B., Jung, O., Precht, C., Kloss, F., Gröbe, A., Heiland, M., & Ebker, T. (2016). Impact of Dental Implant Surface Modifications on Osseointegration. *Biomed Res Int*, 2016, Article 6285620.

Sun, F., Lv, L. T., Cheng, W., Zhang, J. L., Ba, D. C., Song, G. Q., & Lin, Z. (2021). Effect of



Loading Angles and Implant Lengths on the Static and Fatigue Fractures of Dental Implants. *Materials (Basel)*, 14(19), Article 5542.

Won, H.-Y., Choi, Y.-S., & Cho, I.-H. (2010). Effect of Implant Types and Bone Resorption on the Fatigue Life and Fracture Characteristics of Dental Implants. *Journal of Dental Rehabilitation and Applied Science*, 26, 121-143.

ABSTRACT IN KOREAN

추가적인 표면 처리가 적용된 SLA 기반 티타늄 치과 임플란트의 기계적 성능에 관한 비교 연구

본 연구는 sandblasted, large-grit, acid-etched(SLA) 처리된 상용 순수 티타늄 임플란트에 추가적인 표면 처리가 기계적 성능에 통계적으로 유의미한 차이를 유발하는지 평가하고자 하였다.

동일한 치수(직경 3.75 mm, 길이 10 mm)와 내부 육각구조 연결 유형을 가진 33 개의 임플란트-지대주 구성품을 세 그룹으로 나누어 다음과 같이 시험하였다: 그룹 A(대조군; TSIII SA Implant, 오스템임플란트; SLA 처리 표면), 그룹 B(TSIII BA Implant, 오스템임플란트; SLA 처리 표면에 하이드록시아파타이트(hydroxyapatite, HA) 및 포도당 식염액 코팅), 그룹 C(TSIII SOI Implant, 오스템임플란트; SLA 처리 표면에 하이드록시에틸 피페라진에탄설휘산(hydroxyethyl piperazine ethane sulfonic acid, HEPES) 용액 코팅). ISO 14801:2016 표준에 따라 정적 압축 시험과 동적 하중 시험을 수행하였다.

본 연구에서 정적 압축 강도는, 그룹 A 488.7 ± 17.23 N, 그룹 B 456.4 ± 8.82 N, 그룹 C 488.8 ± 31.27 N로 각각 측정되었다. 세 그룹 간 정적 압축 강도에는 통계적으로 유의미한 차이는 관찰되지 않았으며 ($p > 0.05$), 이는 SLA 표면 처리 외 추가적인 표면 개질이 정적 기계적 성능을 크게 향상시키지 못했음을 시사한다. 임상적 저작 조건을 모사한 동적 압축 시험에서는 그룹 A는 210 N(정적 하중의 43%), 그룹 B는 233 N(정적 하중의 51%), 그룹 C는 210 N(정적 하중의 43%)에서 5×10^6 횟수를 견뎌냈다. 이러한 결과는 주요 규제 기관의 요구 사항을 충족하는 피로 한계를 확립한다. 동적 하중 시험 결과, 모든 임플란트 조립체에서



가장 약한 지점은 일관되게 공칭 골 높이에서 근침 방향 3 mm에 위치했으며, 이는 변연골 손실 3 mm를 모방하는 고정 영역에 해당한다.

본 연구 결과에 따르면, SLA 표면처리에 덧붙여진 다양한 표면 처리는 티타늄 임플란트의 정적 및 동적 기계적 특성에 유의미한 영향을 미치지 않았다. 모든 시험된 임플란트는 규제 기준을 상회하는 성능을 보였으며, 이는 생물학적 골유착을 향상시키기 위한 다양한 표면 처리가 임플란트의 기계적 안정성을 손상시키지 않고 적용될 수 있음을 시사한다.

핵심 되는 말: 치과 임플란트, 표면 처리, 기계적 특성, 전단 압축 하중, 피로 한계